# Supplementary Information for: Stratified suppression of turbulence in an ice shelf basal melt parameterisation

Claire K. Yung[1,2,3], Madelaine G. Rosevear[2,4], Adele K. Morrison[1,2], Andrew McC. Hogg[1,3], and Yoshihiro Nakayama[5]

[1]Research School of Earth Sciences, Australian National University, Canberra, Australia
[2]Australian Centre for Excellence in Antarctic Science, University of Tasmania, Hobart, Australia
[3]Australian Centre of Excellence for Climate Extremes, Australian National University, Canberra, Australia
[4]Department of Mechanical Engineering, University of Melbourne, Melbourne, Australia
[5]Institute of Low Temperature Science, Hokkaido University, Hokkaido, Japan

**Correspondence:** Claire Yung (claire.yung@anu.edu.au)

## S1 Tidal Velocities

Fig. S1 shows the velocity variation at the ice-ocean interface in the explicit tide experiments.

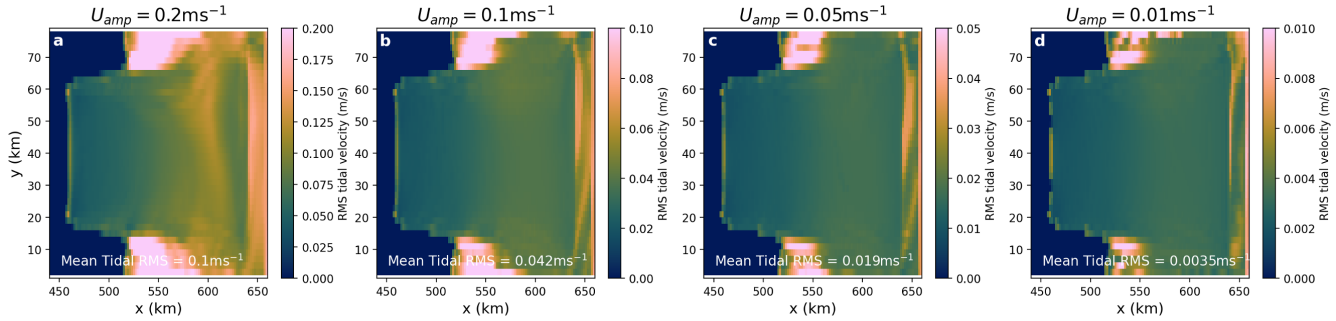


**Figure S1.** RMS tidal velocity at the ice-ocean boundary, computed as $\sqrt{(u-\overline{u})^2+(v-\overline{v})^2}$ from hourly averaged velocities in the last 180 days of the experiment ($u$, $v$), where the overline indicates an average over the 30 days. This was computed for each of the ConstCoeff warm tidal MOM6 experiments with prescribed boundary amplitudes of (a) 0.2 m s$^{-1}$, (b) 0.1 m s$^{-1}$, (c) 0.05 m s$^{-1}$, and (d) 0.01 m s$^{-1}$. Values averaged over the ice shelf cavity are listed in each panel.

## S2 Pine Island Glacier Simulation Additional Figures

Here, we present further supplementary figures of the Pine Island Glacier simulation and compare the hydrography and ocean circulation between experiments with different melt parameterisations. We mainly compare the HJ99-neutral and StratFeedback with tuned drag coefficient experiments since they have similar mean melt rates.

Fig S2a demonstrates the large thermal driving present at Pine Island Glacier, as well as a significant difference in water properties between the ice shelf cavity and open ocean (Fig S2b-d). With the StratFeedback and tuned drag coefficient parameterisation, the ice shelf boundary layer generally warms and becomes more saline, though there is spatial variability. The AB transect along the cavity shows regions of the ice shelf with cooler and warmer boundary layers, and an open ocean sub-surface cooling signal (Fig. S3c,f). The CD transect across the cavity shows similar spatial variability in hydrography changes (Fig. S4c,f), with warming and salinification near the side-walls of the cavity where flows are generally weaker (Fig. 10e) and melt rates are reduced (Fig. 10d) compared to the HJ99-neutral simulation. There are minor differences in the east-southeastern velocity (which approximates the across-CD velocity) compared to HJ99-neutral (Fig. S4i).

However, changes in hydrography and circulation are much stronger between the StratFeedback without drag coefficient tuning and HJ99-neutral experiments. Transects along the cavity show a strong warming and salinification with the StratFeedback parameterisation (Fig. S3b,e), which can be explained by the decreased melt rate and therefore freshwater flux compared to HJ99-neutral (Fig. 10b). The transect across the cavity (Fig. S4b,e,h) shows similar warming and salinification, as well as a weakening flow speed in the cavity, highlighting the importance of buoyant meltwater in generating ocean currents.

Nakayama et al. (2019) compared a similar MITgcm model (same resolution but larger domain) to *in situ* observations along a path similar to our AB transect, finding the simulated Circumpolar Deep Water to be $\sim$0.3°C warmer than observations and the thermocline depth $\sim$100m shallower than observations. Neither metric appears to have significantly improved with the tuned StratFeedback parameterisation (Fig. S3).

Fig. S5a compares the distribution of melt rates between the three tested parameterisations, as well as melt rates computed from the Adusumilli et al. (2020) and Zinck et al. (in review) satellite-derived melt rate products. Whilst not directly comparable, due to different resolutions and missing data (e.g. at the grounding line, where the grounding line is taken from Morlighem et al. (2020), see Figs. S5b,c), the tuned StratFeedback parameterisation (blue colours) has a larger positive melt rate tail than the HJ99-neutral experiment (pink colours), therefore better simulating the large melt rates observed near the grounding line in satellite products (black and grey colours, Adusumilli et al., 2020; Shean et al., 2019; Zinck et al., in review). Note the two satellite products differ significantly, highlighting the uncertainty in satellite-derived melt rates, and the time periods of the satellite products and model run also differ.

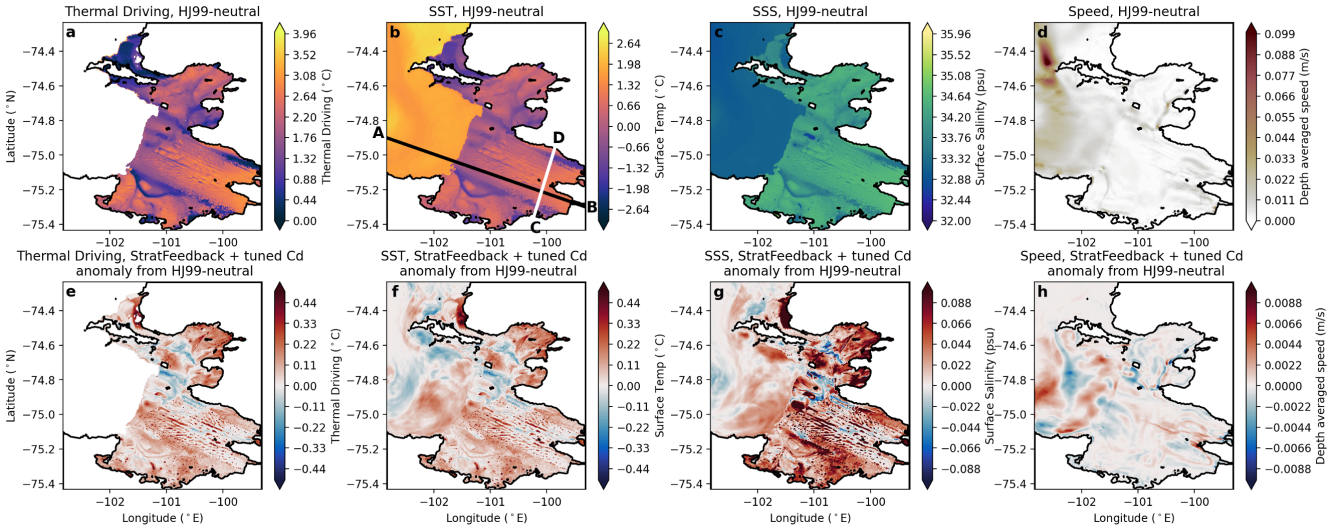


**Figure S2.** Pine Island Glacier model hydrography, showing results averaged over days 20-50 for the HJ99-neutral simulation (top) and average anomaly of the StratFeedback+tuned drag coefficient compared to HJ99-neutral (bottom). The first column shows the thermal driving $T^*$, second the sea surface temperature (using the uppermost cell in the cavity), third the sea surface salinity, and fourth the vertically averaged speed. The black and white lines in panel b are used for Figs. S3 and S4 respectively.

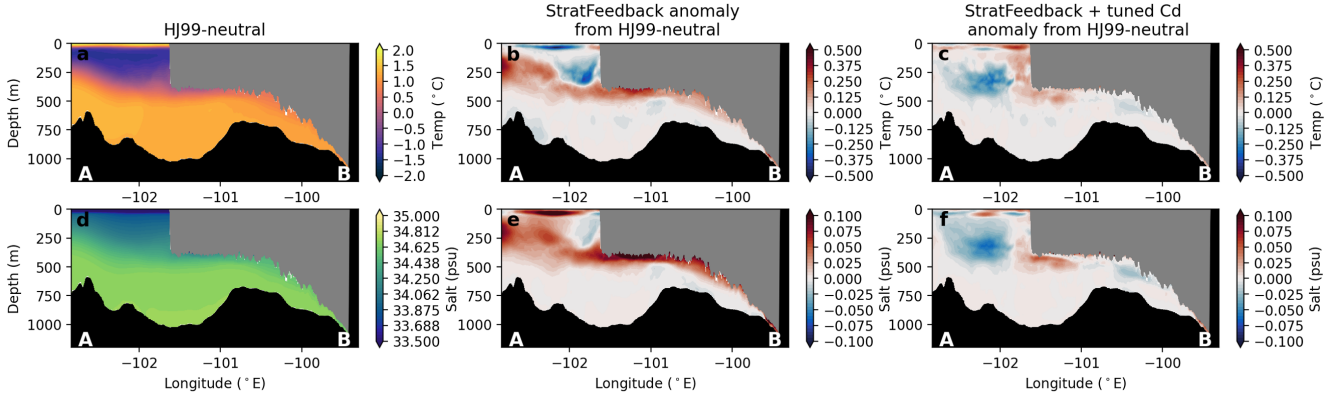


**Figure S3.** Transect along the black AB line of Fig. S2b, averaged over days 20-50 of the simulation. The left column shows the mean for the HJ99-neutral simulation, and the second and third columns show the anomalies for the StratFeedback parameterisation and StratFeedback+tuned drag coefficient parameterisation. Panels a-c show temperature and d-f salinity.

.

.

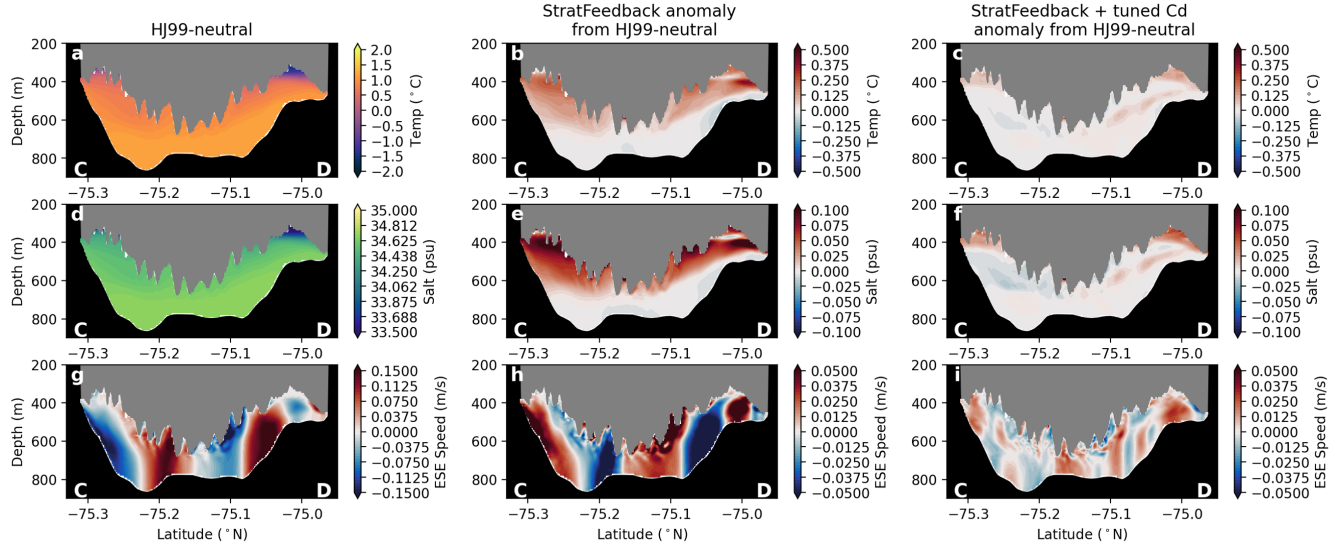


**Figure S4.** Transect along the white CD line of Fig. S2b, averaged over days 20-50 of the simulation. The left column shows the mean for the HJ99 simulation, and the second and third columns show the anomalies for the StratFeedback parameterisation and StratFeedback+tuned drag coefficient parameterisation. Panels a-c show temperature, d-f salinity and g-i east-southeastern velocity (as in Nakayama et al., 2021)

.

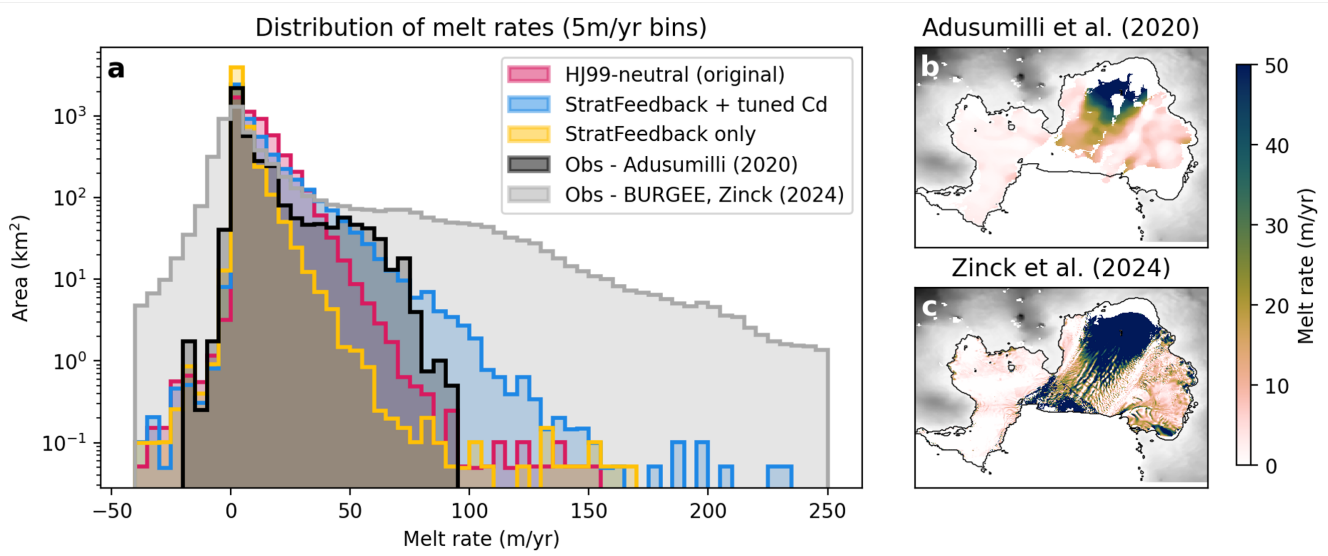


**Figure S5.** (a) Melt rate statistical distributions in Pine Island Glacier, for the MITgcm simulation with three different basal melt parameterisations compared with Adusumilli et al. (2020) (data: Adusumilli et al.) and Zinck et al. (in review) (data: Zinck et al., 2024). Note that the Adusumilli et al. (2020) product is coarser-resolution (500 m) than the MITgcm model (200 m) and is missing data whilst Zinck et al. (in review) is finer resolution (50 m). The $y$-axis is logarithmically scaled. MITgcm data is averaged over simulation days 20-50. (b) Adusumilli et al. (2020) melt rate and (c) Zinck et al. (in review) melt rates at Pine Island Glacier, with the same colourbar as Fig. 10a-c, but note it is rotated with the Antarctic Ice Sheet at the top of the figure and ocean at the bottom. The Bedmachine V3 surface elevation (Morlighem et al., 2020) (data: Morlighem, 2022) is shown in grey and the associated ice shelf mask is outlined with a black contour. Data from Adusumilli et al. is licensed under CC BY 4.0 (https://creativecommons.org/licenses/by/4.0/) and Zinck et al. (2024) is licensed under CC BY-SA 4.0 (https://creativecommons.org/licenses/by-sa/4.0/) and have been adapted in this Figure.

## References


Adusumilli, S., Fricker, H. A., Medley, B. C., Padman, L., and Siegfried, M. R.: Data from: Interannual variations in meltwater input to the Southern Ocean from Antarctic ice shelves., UC San Diego Library Digital Collections., https://doi.org/10.6075/J04Q7SHT.

Adusumilli, S., Fricker, H. A., Medley, B., Padman, L., and Siegfried, M. R.: Interannual variations in meltwater input to the Southern Ocean from Antarctic ice shelves, Nature Geoscience, 13, 616–620, https://doi.org/10.1038/s41561-020-0616-z, 2020.

Morlighem, M.: MEaSUREs BedMachine Antarctica, Version 3., https://doi.org/10.5067/FPSU0V1MWUB6, accessed 22 October 2024, 2022.

Morlighem, M., Rignot, E., Binder, T., Blankenship, D., Drews, R., Eagles, G., Eisen, O., Ferraccioli, F., Forsberg, R., Fretwell, P., et al.: Deep glacial troughs and stabilizing ridges unveiled beneath the margins of the Antarctic ice sheet, Nature Geoscience, 13, 132–137, https://doi.org/10.1038/s41561-019-0510-8, 2020.

Nakayama, Y., Manucharyan, G., Zhang, H., Dutrieux, P., Torres, H. S., Klein, P., Seroussi, H., Schodlok, M., Rignot, E., and Menemenlis, D.: Pathways of ocean heat towards Pine Island and Thwaites grounding lines, Scientific Reports, 9, 16 649, https://doi.org/10.1038/s41598-019-53190-6, 2019.

Nakayama, Y., Cai, C., and Seroussi, H.: Impact of subglacial freshwater discharge on Pine Island Ice Shelf, Geophysical Research Letters, 48, e2021GL093 923, https://doi.org/10.1029/2021GL093923, 2021.

Shean, D. E., Joughin, I. R., Dutrieux, P., Smith, B. E., and Berthier, E.: Ice shelf basal melt rates from a high-resolution digital elevation model (DEM) record for Pine Island Glacier, Antarctica, The Cryosphere, 13, 2633–2656, https://doi.org/10.5194/tc-13-2633-2019, 2019.

Zinck, A.-S. P., Lhermitte, S., Wearing, M., and Wouters, B.: Dataset belonging to the article: Exposure to Underestimated Channelized Melt in Antarctic Ice Shelves, https://doi.org/10.4121/4e2ba9a9-7b1b-4837-b52d-036f8c876e67.v1, 2024.

Zinck, A.-S. P., Lhermitte, S., Wearing, M., and Wouters, B.: Exposure to Underestimated Channelized Melt in Antarctic Ice Shelves, https://doi.org/10.21203/rs.3.rs-4806463/v1, in review.